Earthquakes and Structures, *Vol. 21, No. 2 (2021) 113-124*
https://doi.org/10.12989/eas.2021.21.2.113

Component deformation-based collapse evaluation of RC frame under different collapse criteria

Difang Huang[1a], Xiaolei Han[*1,2], Shengfang Qiao[3], Jing Ji[1,2] and Jidong Cui[4]

[1]*School of Civil Engineering and Transportation, South China University of Technology, Tianhe, Guangzhou, 510641, China;*
[2]*State Key Laboratory of Subtropical Building Science, South China University of Technology, Tianhe, Guangzhou, 510641, China*
[3]*Guangzhou Institute of Building Science Co., Ltd., Guangzhou, 510080, China;*
[4]*RBS Architectural Engineering Design Associates, Guangzhou, 510030, China*

(Received June 13, 2020, Revised April 18, 2021, Accepted May 11, 2021)

Abstract. Developments in performance-based earthquake engineering have emphasized the importance of evaluation of structural collapse resistance. Several collapse criteria were proposed to define structural collapse in various perspective. In this paper, collapse resistant capacity of ductile reinforced concrete (RC) frame was evaluated using different collapse criteria. Since most of the criteria focus on overall structural response, a component deformation-based method was adopted to describe the damage in component level. Incremental dynamic analysis (IDA) of a 6-story ductile RC frame conforms to current codes was conducted in OpenSEES. The collapse resistant capacity under different collapse criteria was compared. Moreover, relationship between overall structural response and the distribution of damaged components were discussed through the component deformation-based method. It was indicated that the story of maximum inter-story drift ratio is neither consistent with the one which is most seriously damaged nor with the story of maximum residual inter-story drift ratio. Furthermore, the component deformation-based method can depict structural damaged state and formation of collapse mechanism more reasonably. The analysis result evidences that structure conforms to current code have the good ductility and hardly reaches physical collapse under rare earthquake, however, the structure is more likely to be demolished due to unacceptable residual deformation.

Keywords: collapse criterion; collapse resistant capacity; component deformation; performance-based earthquake engineering; residual deformation

1. Introduction

The collapse resistant capacity of RC frame structure has drawn great attention from researchers and engineers since RC frame is the most commonly used structural form. However, hazard investigation of past earthquakes indicated that the safety margin of frame structure is relatively low comparing with other structural forms (Kam *et al.* 2011). In order to describe the collapse of structures, several collapse criteria were proposed, which can be mainly divided into two categories: the physical collapse criterion and the indirect collapse criterion. The physical collapse criterion can reflect the actual collapse resistant capacity of structure by simulating the real collapse process. However, it is difficult to simulate the actual collapse state of structure because it is time consuming and not easy to converge in complex structure, which is not suitable for practical engineering. Therefore, the indirect collapse criterion is adopted in most cases. Currently, several indirect collapse criteria have been put forward as follows. (1) The deformation-based criterion: the limit of elastic-plastic inter-story drift for different structures were presented in GB50011-2010 (2016), ASCE 41-06 (2007) and other codes. This definition of collapse was used extensively in practical engineering with certain safety margin. (2) Component failure-based criterion: the collapse of structure is defined when the first failed component appears, such as Shoraka *et al.* (2013) and ASCE 41-17 (2017). (3) Stiffness-based criterion: the reduction of structural stiffness can characterize the failure of structure, and the collapse limit state can be considered when the stiffness degradation reaches a certain extent. The change of tangent stiffness and natural frequency were adopted to describe the structural failure by Gu and Shen (1997), Mohd and Sangle (2017) respectively. (4) Stiffness and deformation-based criterion: the incremental dynamic analysis (IDA) is used to portray the process of structure from elastic state to plastic state, until the structural dynamic instability and side-way mechanism occur, as described in Vamvatsikos and Cornell (2002), FEMA P-695 (2009), Haselton *et al.* (2011), Tian *et al.* (2016), Bayati and Soltani (2016), Qiao *et al.* (2017). (5) Residual deformation-based criterion: the experiences of Mexico earthquake and Kobe earthquake indicate that structures which cannot be repaired have to be demolished due to excessive residual deformation (Ramirez and Miranda 2012). In recent years, more and more researchers have used residual deformation as an index for building resilience assessment (Dai *et al.* 2017, Li *et al.* 2018, Aydemir *et al.* 2019).

At present, the previous research of indirect collapse

*Corresponding author, Professor
E-mail: xlhan@scut.edu.cn
[a]Ph.D. Student
E-mail: rickyhuang8@outlook.com

ISSN: 2092-7614 (Print), 2092-7622 (Online)

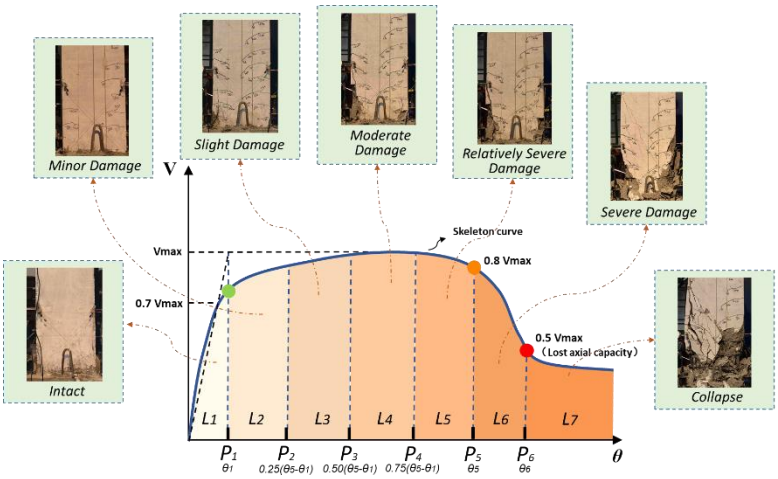

Fig. 1 Component deformation limits and performance levels

criterion focuses mainly on the overall structural response in macro sense like inter-story drift ratio, which is rarely related to the component level in micro sense. However, it is difficult to reflect the actual distribution of structural damage using inter-story drift ratio. In this paper, the component deformation-based method was adopted to study collapse resistant capacity of structure under different collapse criteria, and the relationship between the distribution of damaged components and the collapse criteria was analyzed.

2. Different definitions of collapse

Different collapse criteria describe the collapse state of structure from various perspective and have different safety margin. Collapse criteria commonly used were compared herein.

2.1 Deformation-based criterion

Exceedance of inter-story drift ratio limit is taken as collapse prevention. It is employed extensively in current design standards. The limit of inter-story drift ratio for RC frame is 2.0% in GB50011-2010 (2016), and 1.5~2.5% in ASCE 7-10 (2010). Similarly, ASCE 41-06 (2007) prescribes 4.0% as the limit of collapse prevention.

2.2 First component failure-based criterion

This criterion is proposed in ASCE 41-17 (2017) and Shoraka *et al.* (2013). RC frame is regarded as collapse prevention once failure occurs in structural components. ASCE 41-17 (2017) presented acceptable criteria of different component performance levels including Immediate Occupancy, Life Safety and Collapse Prevention, i.e., IO, LS and CP, for existing buildings. However, a series of research indicated that the criteria are too conservative for most buildings (Acun and Sucuoglu 2010, Siahos and Dritsos 2010, Ricci *et al.* 2012).

Therefore, acceptable criteria of component performance level were modified based on plentiful experimental data by researchers (Qi 2013, Parrotta *et al.* 2014). Base on a test database of 103 RC beams, 469 RC columns and 236 RC shear walls collected from published literatures, Cui (2017) proposed a component deformation-based method to evaluate the performance of RC structures in component level, which is adopted for performance evaluation of RC frame hereinafter. In this method, 6 component deformation limits are established in terms of drift angle, which divides the component performance into 7 states: Intact (L_1), Minor Damage (L_2), Slight Damage (L_3), Moderate Damage (L_4), Relatively Severe Damage (L_5), Severe Damage (L_6) and Collapse (L_7). As illustrated in Fig. 1, deformation limits are defined based on component skeleton curves and three key limits, namely, P_1, P_5, P_6, are the basis of definition. P_1 is the drift angle at normal yielding calculated through the method proposed by Sezen and Moehle (2004), which represents the threshold between elasticity and plasticity. The drift angle at which the applied shear force dropped to 80% of the peak shear force is defined as P_5. Once the component reaches P_5, obvious degradation of lateral bearing capacity occurs but the component still able to stably withstand vertical loads. P_6 is defined as the drift angle corresponding to lost of axial capacity or 50% degradation of lateral bearing capacity. Then P_2, P_3, P_4 are determined by quartering the deformation between P_1 and P_5, as illustrated in Fig.1. Through the regression analysis and systematic experimental verification, Cui *et al.* (2018a, 2018b) put forward new failure mode classification criteria for RC beam, column and shear wall. Han *et al.* (2019) adopted this method in seismic evaluation of a tall building beyond code specification, which proves its rationality and feasibility. Completed component deformation limits adopted here are provided in appendix.

As is introduced in Shoraka *et al.* (2013). one column exceeds performance limit P_6 is considered as collapse prevention in first component failure-based criterion.

2.3 Side-way-based criterion

Side-way collapse is defined as dynamic instability by Vamvatsikos and Cornell (2002). In this criterion, collapse

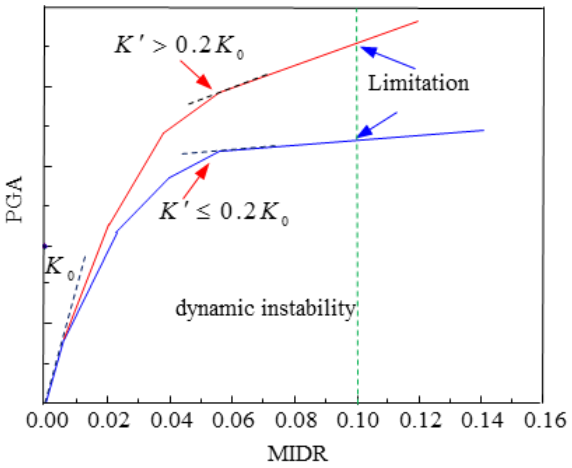

Fig. 2 Side-way collapse mechanism

Table 1 Different collapse criteria

Collapse criterion	No.	Definition of collapse
Deformation-based criterion	C1	MIDR > 2% (GB50011-2010, 2016)
First component failure-based criterion	C2	First column failure
Deformation-based criterion	C3	MIDR > 4% (ASCE41-06, 2006)
Side-way-based criterion	C4	Dynamic instability or storey drift ratio > 10%
Stiffness-based criterion	C5	R_K < 5.0%
Residual deformation-based criterion	C6	RIDR > 1.5%

of structure is defined by two characteristics. First, the maximum inter-story drift ratio (MIDR) increases sharply with the minor ground acceleration increases, which is reflected as the dramatic decline of "story stiffness" represented by the tangent slope of IDA curves, as shown in Eq. (1). Moreover, excessive MIDR in single earthquake excitation also implies the collapse of structure. 10% of MIDR is employed as the threshold. If any of these conditions are met, the structure is regarded as dynamic instability and collapse, as illustrated in Fig. 2.

$$K' \le 0.2K_0 \tag{1}$$

where K_0 is the initial tangent slope of IDA curves when structure remains in elastic range, K' is the tangent slope of IDA curves when structure reaches the capacity point of collapse prevention.

2.4 Stiffness-based criterion

Damage of structure comes with degradation of structural stiffness, therefore, several stiffness-based collapse criteria were put forward by researchers (Sozen and Loopez 1987, Banon and Veneziano 1986, Roufaiel and Meyer 1987). Since stiffness is directly related to dynamic property of structure, Gu (2000) defined the collapse state through structural circular frequency. The collapse appears when the ratio of structural stiffness degradation R_K approaches 0, as shown in Eqs. (2)-(4).

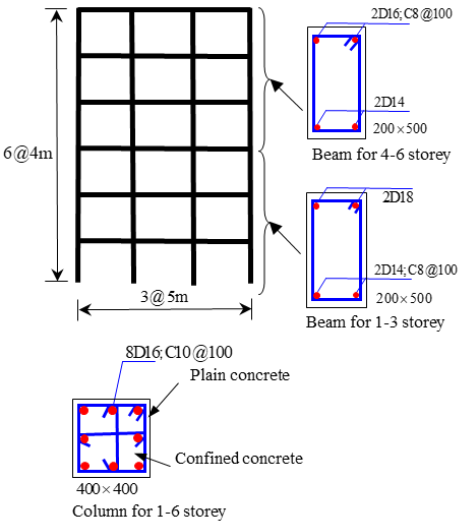

Fig. 3 6-story RC frame (mm)

$$R_K = K / K_0 \approx 0 \tag{2}$$

Where, K_0 and K denote the structural stiffness of original state and collapse prevention separately.

$$K_0 = m\omega_0^2, K = m\omega^2 \tag{3}$$

ω and ω_0 corresponds to the circular frequency. Hence, R_K at collapse prevention can be derived,

$$R_K = K / K_0 = \omega^2 / \omega_0^2 \approx 0 \tag{4}$$

2.5 Residual deformation-based criterion

Through the disaster investigations of earthquakes over the past few decades, researchers found that in many cases although collapse did not occur during earthquake, many RC structures had to be demolished due to expensive repairing cost or loss of repairability caused by excessive residual inter-story drift (RIDR) (Lu *et al.* 2012, Elwood 2013, Ruiz-Pinilla *et al.* 2016). The importance of residual deformation in seismic performance evaluation was realized and several collapse criteria based on residual inter-story drift were proposed (Dai *et al.* 2017, Ruiz-Garc´ıa and Miranda 2006, Hatzigeorgiou *et al.* 2011, Pettinga *et al.* 2007, Ramirez and Miranda 2012). The residual inter-story drift ratio of 1.5% is taken as the median for probability curve of demolition in Ramirez and Miranda (2012), and 1.0% is proposed in FEMA P-58 (2012). The limit of 1.5% was employed herein.

Finally, aforementioned collapse criteria are summarized in Table 1.

3. Numerical examples

3.1 Archetype model

The 2D RC frame structure which conforms to

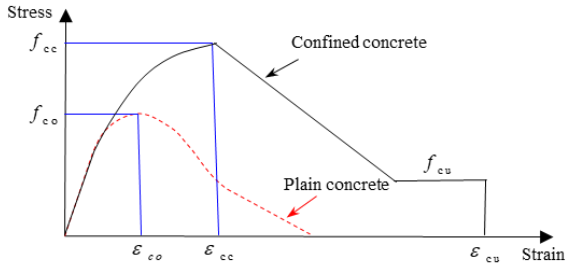

Concrete01 for RC columns
Confined concrete: *-26.1 -0.00328 -7.83 -0.0358*
Plain concrete: *-23.4 -0.00172 -0.00 -0.0040*

Concrete01 for RC beams
Confined concrete: *-21.04 -0.00233 -6.3 -0.0259*
Plain concrete: *-20.1 -0.00164 -0.00 -0.0040*

Fig. 4 Constitutive relation of concrete

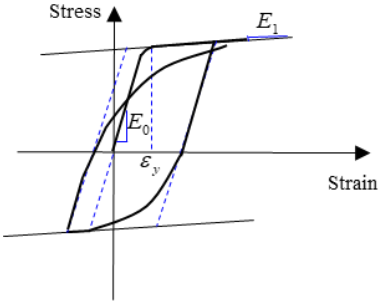

Steel02 for RC elements:
400 206000 0.01 18.5 0.925 0.15 0 1 0 1

Fig. 5 Constitutive relation of steel

GB50011-2010 (2016) is shown in Fig. 3. In order to achieve the design concept of "strong columns and weak beams", "strong shear and weak bending", "strong joints and strong anchoring", specific seismic detailing was adopted, which implies the joint failure will not occur in this model. Uniform distributed load is 19.3 KN/m (including dead and live load) on beams. In addition, mass is 17.6 ton at every beam-column joint connection. Seismic fortification intensity of this building is degree 8 according to GB50011-2010 (2016). Peak ground acceleration (PGA) is 0.07 g and 0.40 g for frequent earthquake and rare earthquake (probability of exceedance is 63.2% and 2% in 50 years) respectively, and site predominant period is 0.35 s. Section information of beams and columns is illustrated in Fig. 3. 8D16 stands for eight rebars whose yield stress is 400MPa and diameter is 16 mm. C10@100 represents stirrup with yield stress of 300 MPa and diameter of 10 mm in a spacing of 100 mm.

3.2 Modeling in OpenSEES

Concrete01 and Steel02 in OpenSEES (2013) were selected as material constitutive model of concrete and reinforcement, which parameters setting is described in Figs. 4 and 5. Furthermore, as illustrated in Fig. 6, fiber section and nonlinearBeamColumn with five integral points along the longitudinal orientation were used for modelling

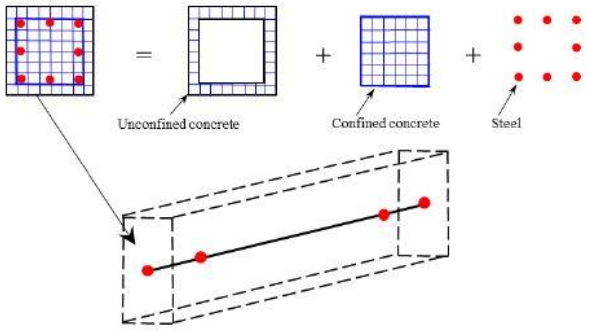

Fig. 6 Fiber section with five Gauss-Lobatto integral points

beams and columns. P-Delta effects was considered in columns. In addition, beam-column connections were assumed to be connected by rigid connection and the bottom columns were fixed on the ground fully.

3.3 Nonlinear time-history analysis

22 earthquake records, which were selected from a set of records proposed in FEMA P-695 (2009), were adopted in time history analysis, as demonstrated in Table 2. The Rayleigh damping of 5% was assumed for the first and second vibration modes. IDA, which was introduced by Vamvatsikos and Cornell (2002), was conducted in OpenSEES (2013). Maximum inter-story drift ratio (MIDR) of each time-history analysis was plotted as one point in Figs. 7(a)-7(b). Thus, a suite of points was presented in Fig. 7(a) under different peak ground accelerations (PGA), and the collapse points defined by different criteria were also marked on the IDA curves. Similarly, the maximum residual inter-story drift ratio (RIDR) can be obtained in Fig. 7(c). The square of circular frequency ω^2 can also be calculated and recorded in Fig. 7(d) when each time-history analysis was finished. g is 10 m/s^2.

3.4 Collapse fragility

The curves of cumulative collapse probability under different collapse criteria can be derived according to Fig. 7(a) and logarithmic curves fitting were obtained in Fig. 8. As illustrated in Fig. 8, in a range of relatively low PGA, the cumulative collapse probability curve for criterion C1 is the steepest, those of C6, C3 and C2 come second, and the curves of C4 and C5 are the flattest, which implies that criterion C1 is most prone to be met, while criterion C4 and C5 are the toughest to reach. However, as the PGA increases, curves of C4 and C5 become steeper while others become flatter. From the increasing trend of these curves, it was indicated that the collapse states defined by C1, C2, C3 and C6 mainly distributed in a range of relatively low PGA, while those defined by C4 and C5 concentrated in a range of high PGA.

In a physical sense, side-way-based criterion (C4) is the closest state of actual collapse. However, from the perspective of economics, loss of repairability or overpriced repairing cost also means failure of structure. According to residual deformation-based criterion (C6), residual inter-

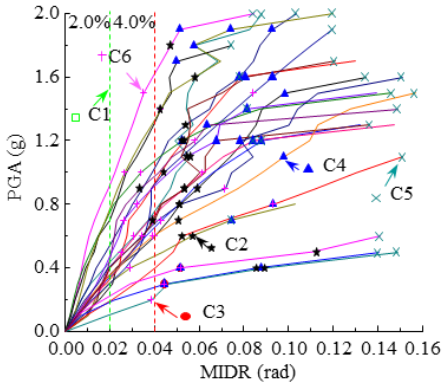

(a) IDA curves of MIDR

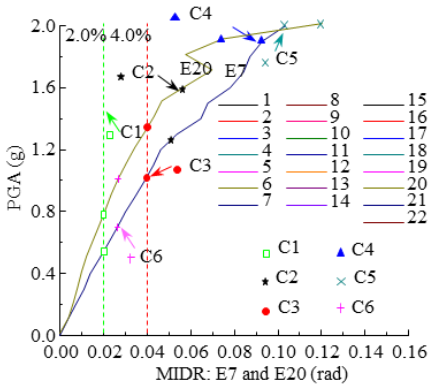

(b) IDA curves of MIDR of E7 and E20

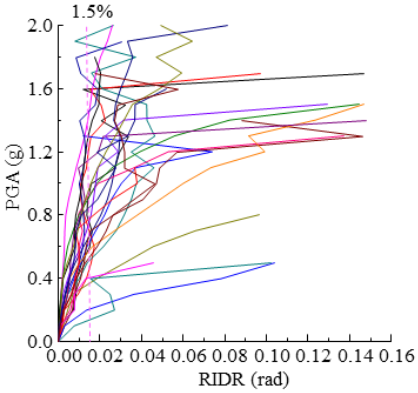

(c) IDA curves of RIDR

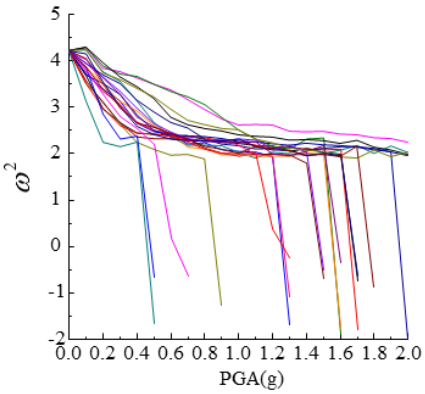

(d) IDA curves of ω^2

Fig. 7 IDA Curves

story drift ratio (RIDR) of 1.5% corresponds to the median in the curve of cumulative demolition probability, which means demolishing is more economic than repairing when the RIDR of structure exceeds 1.5%. Therefore, as illustrated in Fig. 9, based on cumulative probability curves of C4 and C6, post-earthquake state of structures can be divided into three parts, namely, repairability, demolition and collapse. As can be seen in Fig. 9, when RC frame structures which conform building code suffer the rare earthquake (PGA=0.40 g), the probability of reaching criterion C4 is 6.6%. However, there is a demolishing probability of up to 13.5%, which is more than two times of that of side way collapse (C4). And the demolishing probability increases firstly and decreases later as the PGA increases. In other words, although many structures avoid collapsing because of good ductility, they are more likely to be considered as unrepairable and demolished after the earthquake due to excessive residual deformation.

The corresponding PGAs under cumulative collapse probability of 10% and 50% are summarized in Table 3. Collapse probability under different seismic level can also be established in Table 4. Collapse margin ratio (CMR) proposed by FEMA P-695 (2009) was adopted to evaluate the collapse resistance of structure, which can be calculated by Eq. (5).

$$CMR = \frac{S_a(T_1)_{50\%}}{S_a(T_1)_{rare}} \tag{5}$$

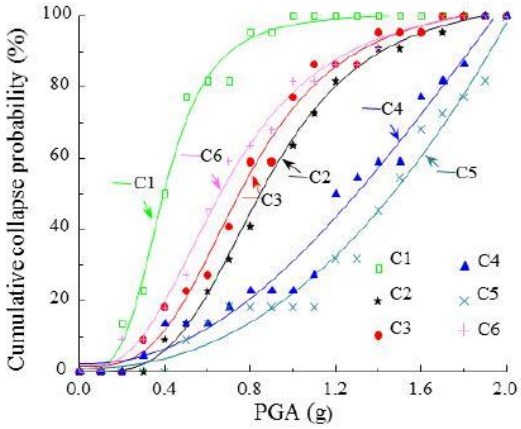

Fig. 8 Cumulative collapse probability under different collapse criteria

where $S_a(T_1)_{50\%}$ is the median spectral acceleration of the collapse level ground motions, $S_a(T_1)_{rare}$ is the spectral acceleration of the rare earthquake ground motions.

According to Table 3, the CMR of criterion C2, C3, C4, C5, C6 increases 119.0%, 76.2%, 152.4%, 219.0%, 119.0% and 115.4%, 92.3%, 233.3%, 274.4%, 59.0% than criterion C1 when the cumulative collapse probability reaches 10% and 50% respectively. The criterion C1 is the most conservative, criterion C2, C3 and C6 come second, which is consistent with Fig. 8. The same trend can also be proved

Table 2 Earthquake records of IDA

Record	Event	Year	Abbreviation	Duration(s)
SFERN/PEL090	San_Fernando	1971	E1	15
SFERN/PEL180	San_Fernando	1971	E2	15
FRIULI/A-TMZ000	Friuli-Italy	1976	E3	15
IMPVALL/H-DLT262	Imperial_Valley	1979	E4	15
IMPVALL/H-E11140	Imperial_Valley	1979	E5	15
SUPERST/B-ICC000	Superstition_Hills	1987	E6	15
SUPERST/B-POE270	Superstition_Hills	1987	E7	15
LOMAP/CAP000	Loma_Prieta	1989	E8	15
LOMAP/G03000	Loma_Prieta	1989	E9	15
CAPEMEND/RIO270	Cape_Mendocino	1992	E10	15
LANDERS/YER270	Landers	1992	E11	15
LANDERS/CLW-LN	Landers	1992	E12	15
NORTHR/MUL009	Northridge	1994	E13	15
NORTHR/LOS000	Northridge	1994	E14	15
KOBE/NIS000	Kobe-Japan	1995	E15	15
KOBE/SHI000	Kobe-Japan	1995	E16	15
KOCAELI/DZC180	Kocaeli-Turkey	1999	E17	15
KOCAELI/ARC000	Kocaeli-Turkey	1999	E18	15
CHICHI/CHY101-E	Chi-Chi-Taiwan	1999	E19	15
CHICHI/TCU045-E	Chi-Chi-Taiwan	1999	E20	15
DUZCE/BOL000	Duzce-Turkey	1999	E21	15
HECTOR/HEC000	Hector_Mine	1999	E22	15

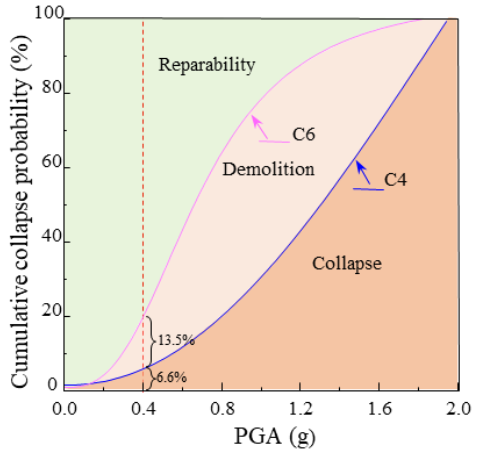

Fig. 9 The post-earthquake states of structure

Table 3 Collapse resistant capacity under different collapse criteria

	C1	C2	C3	C4	C5	C6
PGA(10%)	0.21 g	0.46 g	0.37 g	0.53 g	0.67 g	0.30 g
CMR_1	0.53	1.15	0.93	1.33	1.68	0.75
PGA(50%)	0.39 g	0.84 g	0.75 g	1.30 g	1.46 g	0.62 g
CMR_5	0.98	2.10	1.88	3.25	3.65	1.55

Table 4 Collapse probability under different seismic levels

Seismic level	C1	C2	C3	C4	C5	C6
Frequent (0.07 g)	0.0%	0.0%	0.0%	0.0%	0.0%	0.0%
Moderate (0.20 g)	8.5%	0.6%	2.8%	0.0%	0.0%	4.2%
Rare (0.40 g)	52.1%	6.7%	12.2%	6.6%	3.8%	20.1%

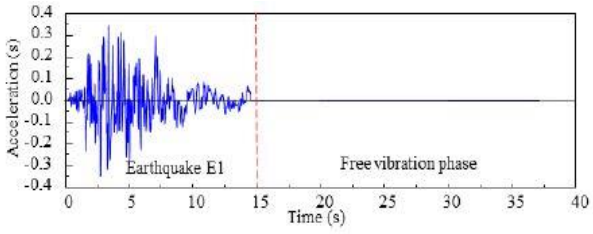

Fig. 10 Time history of Earthquake E1

by Table 4: the collapse probability of criterion C1 is 7.7, 4.3, 7.9, 13.7, 2.6 times of criterion C2, C3, C4, C5, C6 under rare earthquake respectively. It is evidenced that RC frame structure conforms to current codes hardly reach physical collapse state under rare earthquake. However, it is likely to be demolished with a probability of 13.5%, which is also confirmed in Figs. 8 and 9.

3.5 Damaged components distribution under different collapse criteria

Different collapse criteria define the structural collapse state in different aspects, however, most of them focus on the response of overall structure. Component deformation makes it possible to get insight into the structural performance under different collapse criteria. The component deformation limits adopted here for RC beams and columns were derived based on Cui (2017) according to design parameters, as shown in appendix. By applying the deformation limits, yielding mechanism and damaged state of a 6-story frame under different collapse criteria can be described in component level. Structural damage under earthquake E1 and E7 was taken as examples. As shown in Fig. 10, duration of earthquake records is 15 seconds, and the structure vibrates freely from 15 seconds to 40 seconds. The distribution of component damage under each collapse criterion was illustrated in Figs. 11 and 12. And the inter-

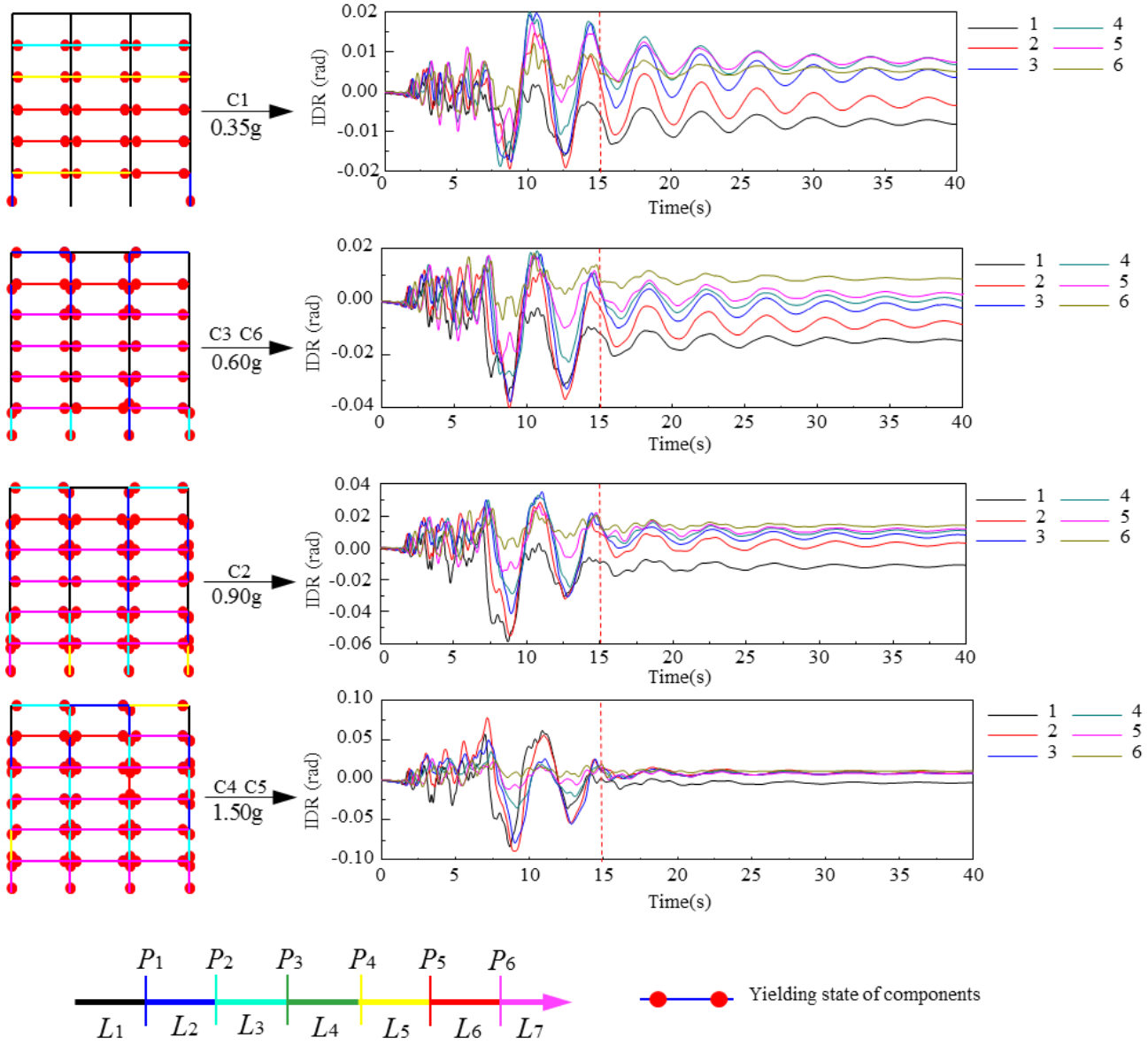

Fig. 11 The distribution of damaged components under E1

story drift ratio (IDR) time history of each story was also presented respectively.

As shown in Fig. 11, when the structure was under excitation of ground motion E1, maximum inter-story drift ratio (MIDR) approaches 2% when *PGA* is 0.35 g, which is at fourth story. Thus, the criterion C1 was reached first. Most beams yielded and reached performance level L_5 and L_6, nevertheless, only two columns yielded and reached L_2. Beam yielding mechanism was formed under this seismic intensity. When *PGA* was 0.60 g, the criterion C3 and C6 reached simultaneously. Almost all of the beams were in L_7. At the same time, all columns of the first story yielded, most of them were in L_3, which means Slight Damage. And the columns in the rest stories generally remained in L_1. Component performance shown that first story was most severely damaged, while MIDR was at the second story. Maximum residual inter-story drift ratio (RIDR) was also at the first story. When *PGA* was 0.90 g, the first column reached L_7 at the first story, which means criterion C2 was met. The MIDR was at the first story, while RIDR was at the sixth story. When *PGA* reached 1.50 g, criterion C4 and C5 ware attained. All of the columns in first story reached L_7 therefore side-way mechanism was formed in first story, which leads to steeply drop of structural stiffness and side-way collapse. The occurrence order of different collapse criteria is C1-C3/C6-C2-C4/C5 under E1. Similarly, the order is C1-C6-C3-C2-C4-C5 under E7.

According to Figs. 11 and 12, beams yielded first, which means structure has the good ductility. The damaged process was captured based on component deformation-based method. The damage extent of columns was slight when criterion C1 was reached first, therefore, C1 is conservative to be considered as collapse criterion.

Similarly, when structure reaches C3, most of the beams

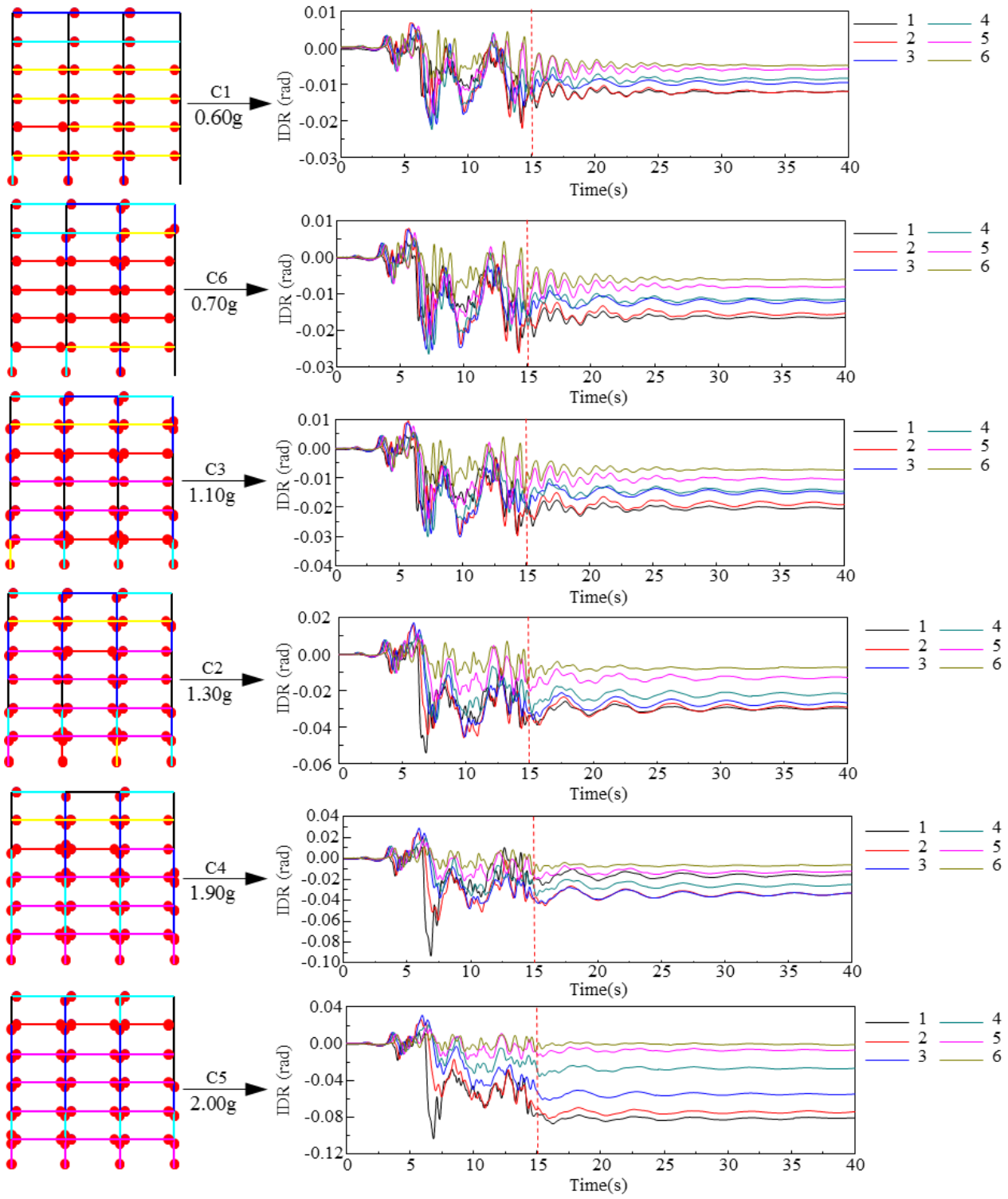

Fig. 12 The distribution of damaged components under E7

suffered serious damaged and reached L_7, but the columns still remained in L_3. Criterion C2 was reached once the first column failure occurs, that is to say, reaching L_7 in component deformation-based method. Actually, the internal force will redistribute when a column failed, thus the remaining columns are still able to withstand the vertical load so that the structure will not collapse. C4 and C5 are the most difficult to reach, but once they are reached, the damage extent is severe. The side-way mechanism formed in one or several stories when structure collapses. Therefore, to a certain extent, criterion C4 and C5 can reflect the true collapse resistant capacity of structure. Moreover, the criterion C4 and C5 are close to each other. Further, C6 is more prone to achieve than C4 and C5, which

indicates the structure is more likely to be demolished due to unacceptable residual deformation before physical collapse occurs.

Figs. 11 and 12 also shows that in many cases the story of MIDR is not the most seriously damaged one. Furthermore, the stories of MIDR and RIDR are not consistent. However, both of MIDR and RIDR increase simultaneously with PGA enhances. The more serious damaged the structure is, the greater MIDR and RIDR are.

4. Conclusions

Several collapse criteria were discussed, and the collapse resistant capacity of a typical RC frame structure under different criteria was compared. The failure mechanism and the distribution of damaged components corresponding to each collapse criterion were also analyzed. Based on the studies above, the following conclusions can be drawn.

- Criterion C1 is most easily to meet, C2, C3 and C6 come next. When criterion C1 is met, the damage of column is slight, thus C1 tends to be conservative. By neglecting the redistribution of internal force, criterion C2 is also conservative. C4 and C5 are the most difficult to achieve, but achieving C4 or C5 means the formation of side-way mechanism in one or several stories. To a certain extent, structure is close to physical collapse state under C4 and C5 thus they reflect the true collapse resistant capacity of structure.
- Frame structures designed in accordance with current codes have good ductility, and hardly reach physical collapse under rare earthquake. However, analysis of post-earthquake state shown that in most cases structures meet criterion C6 first before C4 or C5, which indicates the structures are more likely to be demolished due to unacceptable residual deformation even if they are not collapsed.
- The story of maximum inter-story drift ratio is neither consistent with the one which suffers the severest damaged nor with the one of maximum residual inter-story drift ratio. Through the component deformation-based method, the distribution of structural damage under different collapse criteria can be reflected clearly, which provides insight into the collapse mechanism for researchers and engineers.

Acknowledgments

The research described in this paper is financially supported by Natural Science Foundation of Guangdong Province (2020A1515010739), Science and Technology Program of Guangzhou (202103000038) and China Postdoctoral Science Foundation (2019M662917).

References

Acun, B. and Sucuoglu, H. (2010), "Performance of reinforced concrete columns designed for flexural under severe displacement cycles", *ACI Struct. J.*, **107**(3), 364-371. https://doi.org/10.14359/51663702

ASCE 41-17 (2017), *Seismic Evaluation and Retrofit Rehabilitation of Existing Building*, American Society of Civil Engineers; Reston, Virginia, U.S.A.

ASCE 7-10 (2010), *Minimum Design Loads for Buildings and Other Structures*. American Society of Civil Engineers; Reston, Virginia, U.S.A.

ASCE/SEI 41-06 (2007), *Seismic Rehabilitation of Existing Buildings*. American Society of Civil Engineers; Reston, Virginia, U.S.A.

Aydemir, M.E. and Aydemir, C. (2019), "Residual displacement estimation of simple structures considering soil structure interaction", *Earthq. Struct.*, **16**(1), 69-82. https://doi.org/10.12989/eas.2019.16.1.069

Banon, H. and Veneziano, D. (1986), "Seismic safety of reinforced concrete members and structures", *Earthq. Eng. Struct. Dyn.*, **10**(2), 179-193. https://doi.org/10.1002/eqe.4290100202.

Bayati, Z. and Soltani, M. (2016), "Ground motion selection and scaling for seismic design of RC frames against collapse", *Earthq. Struct.*, **11**(3), 445-459. https://doi.org/10.12989/eas.2016.11.3.445

Cui, J. (2017), Research and Experimental Verification of Deformation Index Limits of RC Beams, Columns and Shear Walls", Ph.D. Dissertation, South China University of Technology, Guangzhou, China.

Cui, J.D. Han, X.L. Ji, J. and Gong, H.J. (2018a), "Experimental study on deformation limits of RC beams", *J. Harbin Institut Technol.*, **50**(6), 169-176. https://doi.org/10.11918/j.issn.0367-6234.201706082.

Cui, J.D., Han, X.L., Gong, H.J. and Ji, J. (2018b), "Deformation limits of reinforces concrete columns and their experimental verification", *J. Tongji Univ. (Nat. Sci.)*, **46**(5), 593-603. https://doi.org/10.11908/j.issn.0253-374x.2018.05.005.

Dai, K., Wang, J., Li, B. and Hong, H.P. (2017), "Use of residual drift for post-earthquake damage assessment of RC buildings", *Eng. Struct.*, **147**, 242-255. https://doi.org/10.1016/j.engstruct.2017.06.001

Elwood, K.J. (2013), "Performance of concrete buildings in the 22 February 2011 Christchurch earthquake and implications for Canadian codes", *Canadian J. Civil Eng.*, **40**, 759-776. https://doi.org/10.1139/cjce-2011-0564

FEMA P-58 (2012), *Seismic Performance Assessment of Buildings*, Federal Emergency Management Agency; Washington, U.S.A.

FEMA P-695 (2009), *Quantification of Building Seismic Performance Factors*, Federal Emergency Management Agency, Washington, U.S.A.

GB50011-2010 (2016), *Code for Seismic Design of Buildings*, Ministry of Housing and Urban-Rural Development of the People's Republic of China, Beijing, China.

Gu, X. and Du, F. (2002), *Computer Simulation of Concrete Structures*. Tongji University Press, Shanghai, China.

Gu, X. and Shen, Z. (1997), "Damage analysis of reinforced concrete structures under earthquake series", *Proceedings of the 7th International Conference on Computing in Civil and Building Engineering*. Seoul, Korea.

Han, X., Huang, D., Ji, J. and Lin, J. (2019), "Component deformation-based seismic design method for RC structure and engineering application", *Earthq. Struct.*, **16**(5), 575-588. https://doi.org/10.12989/eas.2019.16.5.575

Haselton, C.B., Liel, A.B. and Deierlein, G.G., Dean, B.S. and Chou, J.H. (2011), "Seismic collapse safety of reinforced concrete buildings. I: Assessment of ductile moment frames", *J. Struct. Eng.*, **137**(4), 481-491. https://doi.org/10.1061/(ASCE)ST.1943-541X.0000318

Hatzigeorgiou, G.D., Papagiannopoulos, G.A. and Beskos, D.E. (2011), "Evaluation of maximum seismic displacements of SDOF systems from their residual deformation", *Eng. Struct.*, **33**, 3422-3431. https://doi.org/10.1016/j.engstruct.2011.07.006.

Kam, W.Y., Pampanin, S. and Elwood K. (2011), "Seismic performance of reinforced concrete building in the 22 February Christchurch (Lyttelton) earthquake", *Bull. New Zealand Soc. Earthq. Eng.*, **44**(4), 239-278. https://doi.org/10.5459/bnzsee.44.4.239-278.

Li, L., Li, H. and Li, C. (2018), "Seismic fragility assessment of self-centering RC frame structures considering maximum and residual deformations", *Struct. Eng. Mech.*, **68**(6), 677-689. https://doi.org/10.12989/sem.2018.68.6.677.

Lu, X., Ye, L., Ma, Y. and Tang, D. (2012), "Lessons from the collapse of typical RC frames in Xuankou school during the great Wenchuan earthquake", *Advan. Struct. Eng.*, **15**(1), 139-153. https://doi.org/10.1260/1369-4332.15.1.139.

Mohd, M.Z. and Sangle, K.K. (2017), "Seismic damage assessment of reinforced concrete structure using non-linear static analyses", *KSCE J. Civil Eng.*, **21**(4), 1319-1330. https://doi.org/10.1007/s12205-016-0541-2

OpenSEES. (2013), *Open System for Earthquake Engineering Simulation*, Berkeley, CA: Pacific Earthquake Engineering Research Center, University of California. (http://opensees.-berkeley.edu.)

Parrotta, J.E., Peiretti, H.C., Gribniak, V. and Caldentey, A.P. (2014), "Investigating deformations of RC beams: experimental and analytical study", *Comput. Concrete*, **13**(6), 799-827. https://doi.org/10.12989/cac.2014.13.6.799

Pettinga, D., Christopoulos, C., Pampanin, S. and Priestley, N. (2007), "Effectiveness of simple approaches in mitigating residual deformations in buildings", *Earthq. Eng. Struct. Dyn.*, **36**, 1763-1783. https://doi.org/10.1002/eqe.717

Qi, Y. (2013), *Research on Deformation Limits of RC Beams, Columns and Shear Walls Based on Material Strain*, Ph.D. Dissertation, South China University of Technology, Guangzhou, China.

Qiao, S.F., Han, X.L., Li, W.C. and Zhou, K.M. (2017), "Conceptual configuration and seismic performance of high-rise steel braced frame", *Steel Compos. Struct.*, **23**(2), 173-186. https://doi.org/10.12989/scs.2017.23.2.173.

Ramirez, C.M. and Miranda, E. (2012), "Significance of residual drifts in building earthquake loss estimation", *Earthq. Eng. Struct. Dyn.*, **41**(11), 1477-1493. https://doi.org/10.1002/eqe.2217.

Ricci, P., Verderame, G. and Manfredi, G. (2012), "ASCE/SEI 41 provisions on deformation capacity of older-type reinforced concrete columns with plain bars", *J. Struct. Eng.*, **139**(12), 04013014. https://doi.org/10.1061/(asce)st.1943-541x.0000701.

Roufaiel M.S. and Meyer C. (1987), "Analytical model of hysteretic behavior of RC frames", *J. Struct. Eng.*, **113**(3), 429-444. https://doi.org/10.1061/(ASCE)0733-9445(1987)113:3(429).

Ruiz-Garc´ıa, J. and Miranda, E. (2006), "Evaluation of residual drift demands in regular multi-storey frames for performance-based seismic assessment", *Earthq. Eng. Struct. Dyn.*, **35**, 1609-1629. https://doi.org/10.1002/eqe.593.

Ruiz-Pinilla, J.G., Adam, J.M., Pérez-Cárcel, R. Yuste, J. and Moragues, J.J. (2016), "Learning from RC building structures damaged by the earthquake in Lorca, Spain, in 2011", *Eng. Fail. Analy.*, **68**, 76-86. https://doi.org/10.1016/j.engfailanal.2016.05.013

Sezen, H. and Moehle, J.P. (2004), "Shear strength model for lightly reinforced concrete columns", *J. Struct. Eng.*, **130**(11), 1692-1703. https://doi.org/10.1061/(asce)0733-9445(2004)130:11(1692)

Shoraka, M.B., Yang, T.Y. and Elwood, K.J. (2013), "Seismic loss estimation of non-ductile reinforced concrete buildings", *Earthq. Eng. Struct. Dyn.*, **42**(2), 297-310. https://doi.org/10.1002/eqe.2213.

Siahos, G. and Dritsos, S. (2010), "Procedural assumption comparison for old buildings via pushover analysis including the ASCE 41 update", *Earthq. Spectra*, **26**(1), 187-208. https://doi.org/10.1193/1.3272266.

Sozen, M.A. and Loopez, R.R. (1987), "RC frame drift for 1985 Mexico earthquake", *The Mexico Earthquakes—1985: Factors Involved and Lessons Learned*, Mexico City, September.

Tian, Y., Lu, X., Lu, X.Z., Li, M.K. and Guan, H. (2016), "Quantifying the seismic resilience of two tall buildings designed using Chinese and US Codes", *Earthq. Struct.*, **11**(6), 925-942. https://doi.org/10.12989/eas.2016.11.6.925.

Vamvatsikos, D. and Cornell, C. (2002), "Incremental dynamic analysis", *Earthq. Eng. Struct. Dyn.*, **31**(3), 491-514. https://doi.org/10.1002/eqe.141.

DK

Appendix

Notation:

λ is shear span ratio of the component, which can be calculated by $\lambda = L_a / h_0 \approx M / Vh_0$.

m is flexural shear ratio of the component, which can be calculated by $m=V_p / V_0 = M_n / V_n L_a$.

L_a is the effective length of the cantilever.

M and V is the moment and shear force at cantilever end.

h_0 is effective height of section, for beam and column equal to the distance between section compression edge and the point of resultant force of tension reinforcement, for shear wall equal to 0.8 times the section height.

M_n is the flexural capacity of RC component.

V_0 is the shear capacity of RC columns and beams according to ACI 318-14.

$V_{n,ACI}$ is the shear capacity of RC shear wall according to ACI 318-14.

V_n is the shear capacity of RC beams, columns and shear walls according to Chinese code GB 50010-2010.

$V/f_{ck}bh_0$ is the nominal shear compression ratio.

f_{ck} is the characteristic value of concrete compressive strength.

b is width of section.

λ_v is stirrup characteristic value of the component, which can be calculated by $\lambda_v = \rho_{volume} f_y / f_c$.

ρ_{volume} is the volume stirrup ratio, for beams and columns, it is calculated according to the stirrup in the component, for shear walls, it is calculated according to the stirrup in boundary elements.

f_y is the yield strength of stirrup.

f_c is the axial compressive strength of concrete.

ρ_t is stirrup ratio along the loading direction.

α is the confinement effectiveness factor in Mander concrete model.

n is the axial load ratio of component, which can be calculated by $n = P / Af_c$.

Table A-1 Failure mode classification criterion of RC beams

Failure mode	Shear span ratio	Flexural shear ratio
Flexural	λ>=2.0	m<=1.0
Shear	λ>=2.0	m>1.0
	λ<2.0	

Table A-2 Failure mode classification criterion of RC columns

Failure mode	Shear span ratio	Flexural shear ratio
Flexural	λ>=2.0	m<=0.6
Flexural-shear	λ>=2.0	0.6<m<=1.0
Shear	λ>=2.0	m>1.0
	λ<2.0	

Table A-3 Deformation limit of RC beams

Design Parameter			Performance level					
			Intact	Minor Damage	Slight Damage	Moderate Damage	Relatively Severe Damage	Severe Damage
Flexural								
m	λ_v	$V/f_{ck}bh_0$						
≤0.2	≥0.2	≤0.02	0.004	0.011	0.023	0.034	0.045	0.050
≤0.2	≥0.2	≥0.1	0.004	0.005	0.010	0.015	0.020	0.025
≥0.8	≥0.2	≤0.02	0.005	0.014	0.028	0.041	0.055	0.060
≥0.8	≥0.2	≥0.1	0.005	0.009	0.018	0.026	0.035	0.040
≤0.2	≤0.02	≤0.02	0.003	0.003	0.007	0.010	0.014	0.015
≤0.2	≤0.02	≥0.1	0.003	0.001	0.001	0.002	0.002	0.002
≥0.8	≤0.02	≤0.02	0.005	0.007	0.014	0.020	0.027	0.032
≥0.8	≤0.02	≥0.1	0.005	0.002	0.004	0.006	0.008	0.010
Shear								
m	ρ_t							
≤0.5	≥0.008		0.004	0.005	0.010	0.015	0.020	0.022
≥2.5	≥0.008		0.004	0.003	0.005	0.008	0.010	0.012
≤0.5	≤0.0005		0.004	0.003	0.005	0.008	0.010	0.012
≥2.5	≤0.0005		0.004	0.001	0.003	0.004	0.005	0.008

Table A-4 Deformation limit of RC columns

Design Parameter			Performance level					
			Intact	Minor Damage	Slight Damage	Moderate Damage	Relatively Severe Damage	Severe Damage
Flexural								
n	$\alpha\lambda_v$	$V/f_{ck}bh_0$						
≤0.1	≥0.4	≤0.02	0.006	0.008	0.015	0.023	0.030	0.044
≤0.1	≥0.4	≥0.1	0.008	0.014	0.028	0.041	0.055	0.060
≥0.6	≥0.4	≤0.02	0.005	0.006	0.012	0.017	0.023	0.025
≥0.6	≥0.4	≥0.1	0.005	0.006	0.012	0.018	0.024	0.028
≤0.1	≤0.02	≤0.02	0.004	0.006	0.012	0.018	0.024	0.028
≤0.1	≤0.02	≥0.1	0.008	0.010	0.020	0.030	0.040	0.048
≥0.6	≤0.02	≤0.02	0.005	0.000	0.000	0.000	0.000	0.000
≥0.6	≤0.02	≥0.1	0.005	0.005	0.009	0.014	0.018	0.022
Flexural-shear								
n	ρ_t	m						
≤0.1	≥0.01	≤0.6	0.008	0.009	0.018	0.027	0.036	0.043
≤0.1	≥0.01	≥1.0	0.008	0.008	0.016	0.024	0.032	0.034
≥0.6	≥0.01	≤0.6	0.003	0.004	0.009	0.013	0.017	0.020
≥0.6	≥0.01	≥1.0	0.003	0.005	0.010	0.015	0.020	0.023
≤0.1	≤0.0005	≤0.6	0.006	0.006	0.013	0.019	0.025	0.031
≤0.1	≤0.0005	≥1.0	0.006	0.003	0.007	0.010	0.013	0.016
≥0.6	≤0.0005	≤0.6	0.002	0.001	0.001	0.002	0.002	0.002
≥0.6	≤0.0005	≥1.0	0.002	0.000	0.000	0.000	0.000	0.000
Shear								
n	ρ_t							
≤0.1	≥0.008		0.004	0.003	0.005	0.008	0.010	0.015
≥0.6	≥0.008		0.004	0.002	0.004	0.006	0.008	0.010
≤0.1	≤0.0005		0.003	0.001	0.002	0.003	0.004	0.004
≥0.6	≤0.0005		0.003	0.000	0.000	0.000	0.000	0.000